J|A|C|S ARTICLES

Published on Web 01/28/2010

# Factors Governing the $Na^+$ vs $K^+$ Selectivity in Sodium Ion Channels

Todor Dudev[†] and Carmay Lim*[,†,‡]

*Institute of Biomedical Sciences, Academia Sinica, Taipei 115, Taiwan, and the Department of Chemistry, National Tsing Hua University, Hsinchu 300, Taiwan*

Received November 2, 2009; E-mail: carmay@gate.sinica.edu.tw

***Abstract:*** Monovalent $Na^+$ and $K^+$ ion channels, specialized pore-forming proteins that play crucial biological roles such as controlling cardiac, skeletal, and smooth muscle contraction, are characterized by a remarkable metal selectivity, conducting the native cation while rejecting its monovalent contender and other ions present in the cellular/extracellular milieu. Compared to $K^+$ channels, the principles governing $Na^+$ vs $K^+$ selectivity in both epithelial and voltage-gated $Na^+$ channels are much less well understood due mainly to the lack of high-resolution 3D structures. Thus, many questions remain. It is not clear if the serines lining the pore of epithelial $Na^+$ channel bind to the metal cation via their backbone or side chain O atoms and why substituting the Lys lining the pore of voltage-gated $Na^+$ channels to another residue such as Arg drastically reduces or even reverses the $Na^+/K^+$ selectivity. This work systematically evaluates the effects of various factors such as (i) the number, chemical type, and charge of the pore's coordinating groups, (ii) the hydration number and coordination number of the metal cation, and (iii) the solvent exposure and the size/rigidity of the pore on the $Na^+$ vs $K^+$ selectivity in model $Na^+$ channel selectivity filters (the narrowest part of the pore) using a combined density functional theory/continuum dielectric approach. The results reveal that the $Na^+$ channel's selectivity for $Na^+$ over $K^+$ increases if (1) the pore provides three rather than four protein ligands to coordinate to the metal ion, (2) the protein ligands have strong charge-donating ability such as Asp/Glu carboxylate or backbone carbonyl groups, (3) the passing $Na^+$ is bare or less well hydrated inside the filter than the competing $K^+$, and (4) the pore is relatively rigid, constricted, and solvent exposed. They also reveal that factors favoring $Na^+/K^+$ selectivity in $Na^+$ channels generally disfavor $K^+/Na^+$ selectivity in $K^+$ channels and vice versa. The different selectivity principles for the $K^+$ and $Na^+$ channels are consistent with the different architecture, composition, and properties of their selectivity filters. They provide clues to the metal-binding site structure in the selectivity filters of epithelial and voltage-gated $Na^+$ channels.

## Introduction

Monovalent $Na^+$ and $K^+$ ions are key players in several processes that ensure normal functioning of living animal organisms. They are involved in regulating (i) the homeostasis of blood and body fluids, (ii) cardiac, skeletal, and smooth muscle contraction, (iii) taste and pain sensation, (iv) hormone secretion, and (v) signal transduction.[1−3] They coexist in different biological compartments with different relative concentrations: $K^+$ is the principal cation in the cytoplasm (the $[K^+]/[Na^+]$ concentration ratio is 139/12 mM), while $Na^+$ dominates the extracellular space (the $[Na^+]/[K^+]$ is 145/4 mM).[4] $Na^+$ and $K^+$ transport across the cell membrane is carried out by specialized pore-forming proteins, ion channels or ion pumps, which, by regulating the inward/outward flow of the respective cation, exert tight control on electrical signals in cells.[2] As $Na^+$ and $K^+$ ions are both present in the body fluids, their respective ion channels should discriminate between the two competing metal ions, conducting the native cation while rejecting its monovalent contender (and other ions present in the cellular/extracellular milieu). Indeed, monovalent ion channels are characterized by remarkable metal selectivity. Potassium channels select $K^+$ over $Na^+$ by a ratio of ~1000:1,[2] whereas the epithelial $Na^+$ channel exhibits a $Na^+/K^+$ selectivity ratio higher than 500:1.[5,6] Both types of channels are inaccessible to anions and exclude divalent cations.[2,7] This striking ion selectivity of monovalent ion channels is astonishing in view of the close similarity between $Na^+$ and $K^+$: both are spherical alkali cations with the same charge, analogous chemical and physical properties, and similar ionic radii (1.02 and 1.38 Å for hexacoordinated $Na^+$ and $K^+$, respectively[8]). Yet, the channel is able to "sense" the native ion and selectively let it pass through.

Unraveling the basic determinants of this remarkable ion channel selectivity has been a subject of extensive investigations using both experimental and theoretical methods. The atomic

[†] Academia Sinica.
[‡] National Tsing Hua University.

(1) Mano, I.; Driscoll, M. *Bioessays* **1999**, *21*, 568–578.
(2) Hille, B. *Ionic Channels of Excitable Membranes*; 3rd ed.; Sinauer Associates: Sunderland, MA, 2001.
(3) Snyder, P. M. *Endocr. Rev.* **2002**, *23*, 258–275.
(4) Voet, D.; Voet, J. G. *Biochemistry*; John Wiley & Sons: New York, 1990.
(5) Benos, D. J. *Am. J. Physiol. Cell. Physiol.* **1982**, *242*, C131–C145.
(6) Palmer, L. G. *J. Membr. Biol.* **1982**, *67*, 91–98.
(7) Schlief, T.; Schonherr, R.; Imoto, K.; Heinemann, S. H. *Eur. Biophys. J.* **1996**, *25*, 75–91.
(8) Shannon, R. D. *Acta Crystallogr. A* **1976**, *32*, 751–767.

structures of several $K^+$ channels by X-ray crystallography[9−19] complemented by insights from theoretical studies[20−34] have elucidated the underlying physical principles governing the $K^+$/$Na^+$ selectivity in these systems. These studies conclude that a rigid pore of precise geometry that fits only $K^+$ but not the smaller $Na^+$ [15,35] does not control ion selectivity in $K^+$ channels.[24,28−30,32] Our recent study showed that $K^+$ channel selectivity for $K^+$ over $Na^+$ increases with (i) increasing number but decreasing magnitude of the coordinating dipoles and (ii) decreasing solvent exposure of the pore, which favors a larger hydration number (HN, number of metal-bound water molecules) of $K^+$ relative to that of $Na^+$.[34] Thus, high $K^+/Na^+$ selectivity could be achieved by (i) a pore lined with eight carbonyl ligands and (ii) finely tuned physicomechanical properties of the channel walls providing a low dielectric medium favoring an octahydrated permeating $K^+$ and enough stiffness to force the competing $Na^+$ to adopt an unfavorable 8-fold coordination.[34]

Compared to $K^+$ channels, the basic principles governing metal selectivity in $Na^+$ channels are less well understood. This is due mainly to the lack of high-resolution structures of $Na^+$ channels and their selectivity filters; i.e., the narrowest part of the pore controlling its metal selectivity. Notably, even the oligomeric state of some classes of $Na^+$ channels has been a subject of heated debate and controversy. For example, using various electrophysiological and biochemical experiments, ion channels belonging to the epithelial $Na^+$ channel/degenerin family have been found to form trimers,[36] tetramers,[37,38] octamers,[39] or even nanomers.[39,40] This long-standing issue has been resolved by the 1.9-Å X-ray structure of an acid-sensing ion channel from the same family, showing that this ion channel is a homotrimer.[41,42] This implies that the other channels in the degenerin family are also formed by three subunits and the epithelial $Na^+$ channel is a heterotrimer with $\alpha_1\beta_1\gamma_1$ stoichiometry.[41,42] Unfortunately, the acid-sensing ion channel was crystallized without metal ions inside the pore, thus the exact location of its selectivity filter and the mode of its interaction with the permeating cation remain unclear.[41]

Information about the composition of $Na^+$ channels' selectivity filters comes mainly from site-directed mutagenesis and channel-blocker binding experiments. Such experiments have strongly suggested that the selectivity filter of the epithelial $Na^+$ channel is lined with conserved Ser residues from the $\alpha$, $\beta$, and $\gamma$ subunits.[43−49] However, there is no consensus about the orientation of the Ser side chains: Kellenberger et al.[47] proposed that the Ser side chains point away from the pore lumen, while their backbone O atoms face the pore and participate in metal binding. In contrast, Sheng et al.[49] proposed that the Ser hydroxyl group from the $\alpha$ subunit points to the pore lumen and interacts with the permeating cation.

The selectivity filter of another class of $Na^+$ channels—the voltage-gated $Na^+$ channels participating in generating action potentials in excitable cells—is even more enigmatic than that of the epithelial $Na^+$ channel. Unlike the latter, these channels are tetrameric rather than trimeric, and the key residues lining the selectivity filter have been identified: The Asp(I), Glu(II), Lys(III), and Ala(IV) residues, one from each of the nonidentical domains I−IV comprising the $Na^+$ channel, form the so-called DEKA motif/locus and are responsible for the channel's ion selectivity.[50−56] Surprisingly, among the four highly conserved residues, Lys, which does not typically bind metal cations, is nevertheless required for $Na^+/K^+$ discrimination: its mutation to another amino acid (aa) residue, even to a positively charged Arg, drastically reduces (or even reverses) the channel's selectivity for $Na^+$.[7,55,57,58] However, how this Lys dictates $Na^+/K^+$ selectivity is not clear (see below). Furthermore, the DEKA Ala side chain orientation with respect to the pore lumen is still subject to controversy: Channel-blocker binding experiments


(9) Doyle, D. A.; Cabral, J. M.; Pfuetzner, R. A.; Kuo, A.; Gulbis, J. M.; Cohen, S. L.; Cahit, B. T.; MacKinnon, R. *Science* **1998**, *280*, 69–67.
(10) Zhou, Y.; Morais-Cabral, J. H.; Kaufman, A.; MacKinnon, R. *Nature* **2001**, *414*, 43–48.
(11) Jiang, Y.; Lee, A.; Chen, J.; Cadene, M.; Chait, B. T.; MacKinnon, R. *Nature* **2002**, *417*, 515–522.
(12) Jiang, Y.; Lee, A.; Chen, J.; Cadene, M.; Chait, B. T.; MacKinnon, R. *Nature* **2002**, *417*, 523–526.
(13) Kuo, A.; Gulbis, J. M.; Antcliff, J. F.; Rahman, T.; Lowe, E. D.; Zimmer, J.; Cuthbertson, J.; Ashcroft, F. M.; Ezaki, T.; Doyle, D. A. *Science* **2003**, *300*, 1922–1926.
(14) Jiang, Y.; Lee, A.; Chen, J.; Ruta, V.; Cadene, M.; Chait, B. T.; MacKinnon, R. *Nature* **2003**, *423*, 33–41.
(15) Gouaux, E.; MacKinnon, R. *Science* **2005**, *310*, 1461–1465.
(16) Shi, N.; Ye, S.; Alam, A.; Chen, L.; Jiang, Y. *Nature* **2006**, *440*, 570–574.
(17) Long, S. B.; Tao, X.; Campbell, E. B.; MacKinnon, R. *Nature* **2007**, *450*, 376–382.
(18) Nishida, M.; Cadene, M.; Chait, B. T.; MacKinnon, R. *EMBO J.* **2007**, *26*, 4005–4015.
(19) Alam, A.; Jiang, Y. *Nature Struct. Mol. Biol.* **2009**, *16*, 30–34.
(20) Eisenman, G. *Biophys. J.* **1962**, *2*, 259–323.
(21) Laio, A.; Torre, V. *Biophys. J.* **1999**, *76*, 129–148.
(22) Åqvist, J.; Luzhkov, V. *Nature* **2000**, *404*, 881–884.
(23) Luzhkov, V. B.; Åqvist, J. *Biochim, Biophys. Acta* **2001**, *1548*, 194–202.
(24) Noskov, S. Y.; Berneche, S.; Roux, B. *Nature* **2004**, *431*, 830–834.
(25) Corry, B.; Vora, T.; Chung, S.-H. *Biochim. Biophys. Acta* **2005**, *1711*, 72–86.
(26) Asthagiri, D.; Pratt, L. R.; Paulaitis, M. E. *J. Chem. Phys.* **2006**, *125*, 24701−1−24701−6.
(27) Corry, B.; Chung, S.-H. *Cell. Mol. Life Sci.* **2006**, *63*, 301–315.
(28) Noskov, S. Y.; Roux, B. *Biophys. Chem.* **2006**, *124*, 279–291.
(29) Bostick, D. L.; Brooks, C. L., III *Proc. Natl. Acad. Sci. U.S.A.* **2007**, *104*, 9260–9265.
(30) Thomas, M.; Jayatilaka, D.; Corry, B. *Biophys. J.* **2007**, *93*, 2635–2643.
(31) Varma, S.; Rempe, S. B. *Biophys. J.* **2007**, *93*, 1093–1099.
(32) Fowler, P. W.; Tai, K.; Sansom, M. S. P. *Biophys. J.* **2008**, *95*, 5062–5072.
(33) Varma, S.; Sabo, D.; Rempe, S. B. *J. Mol. Biol.* **2008**, *376*, 13–22.
(34) Dudev, T.; Lim, C. *J. Am. Chem. Soc.* **2009**, *131*, 8092–8101.
(35) Bezanilla, F.; Armstrong, C. M. *J. Gen. Physiol.* **1972**, *53*, 342–347.
(36) Staruschenko, A.; Adams, E.; Booth, R. E.; Stockand, J. D. *Biophis. J.* **2005**, *88*, 3966–3975.
(37) Coscoy, S.; Lingueglia, E.; Lazdunski, M.; Barbry, P. *J, Biol. Chem.* **1998**, *273*, 8317–8322.
(38) Firsov, D.; Gautschi, I.; Merillat, A.-M.; Rossier, B. C.; Schild, L. *EMBO J.* **1998**, *17*, 344–352.
(39) Eskandari, S.; Snyder, P. M.; Kreman, M.; Zampighi, G. A.; Wellsh, M. J.; Wright, E. M. *J. Biol. Chem.* **1999**, *274*, 27281–27286.
(40) Snyder, P. M.; Cheng, C.; Prince, L. S.; Rogers, J. C.; Welsh, M. J. *J. Biol. Chem.* **1998**, *273*, 681–684.
(41) Jasti, J.; Furukawa, H.; Gonzales, E. B.; Gouaux, E. *Nature* **2007**, *449*, 316–324.
(42) Canessa, C. M. *Nature* **2007**, *449*, 293–294.
(43) Kellenberger, S.; Gautshi, I.; Schild, L. *Proc. Natl. Acad. Sci. U.S.A.* **1999**, *96*, 4170–4175.
(44) Kellenberger, S.; Hoffmann-Pochon, N.; Gautschi, I.; Schneeberger, E.; Schild, L. *J. Gen. Physiol.* **1999**, *114*, 13–30.
(45) Snyder, P. M.; Olson, D. R.; Bucher, D. B. *J. Biol. Chem.* **1999**, *274*, 28484–28490.
(46) Sheng, S.; Li, J.; McNulty, K. A.; Avery, D.; Kleyman, T. R. *J. Biol. Chem.* **2000**, *275*, 8572–8581.
(47) Kellenberger, S.; Auberson, M.; Gautschi, I.; Schneeberger, E.; Schild, L. *J. Gen. Physiol.* **2001**, *118*, 679–692.
(48) Kellenberger, S.; Schild, L. *Physiol. Rev.* **2002**, *82*, 735–767.
(49) Sheng, S.; Perry, C. J.; Kashlan, O. B.; Kleyman, T. R. *J. Biol. Chem.* **2005**, *280*, 8513–8522.

on Cys-substituted single mutants of the DEKA motif suggest that the respective selectivity filter side chains, including Ala, point inward to the conduction pore.[59] However, structures derived from molecular dynamics simulations of modeled wild-type and mutant voltage-gated $Na^+$ channels show that it is the Ala backbone carbonyl group that is exposed to the pore.[60,61]

Two hypotheses—"static" and "dynamic"—compete to plausibly explain the mechanism of $Na^+$ vs $K^+$ selectivity in voltage-gated $Na^+$ channels. In the static hypothesis, Favre et al.,[55] based on a plethora of mutagenesis studies, speculated that the positively charged Lys ammonium could form a strong salt bridge with the negatively charged Asp/Glu carboxylate from the DEKA locus. This could constrain the pore size to dimensions that accommodate $Na^+$ better than $K^+$ or orient the coordinating O atoms to better suit the $Na^+$ coordination requirements. In the dynamic hypothesis, Lipkind and Fozard,[60,61] based on modeling studies of voltage-gated $Na^+$ channels, proposed that the two acidic residues of the DEKA filter interact with the neighboring Lys in the metal-free filter. Since $Na^+$ is a stronger Lewis acid than $K^+$ (with its higher charge/size ratio), it can compete with the lysine's $-NH_3^+$ to bind to Glu/Asp, whereas $K^+$ cannot displace Lys from its interactions with the carboxylates and thus cannot pass through the pore. Thus, selectivity is determined by the pore size/rigidity in the static hypothesis but by the ability of the permeating ion to compete with lysine's $-NH_3^+$ for the $COO^-$ moieties in the dynamic hypothesis.

The above summary of our current knowledge on the determinants of metal selectivity in $Na^+$ channels raises the following intriguing questions: (1) Other than the pore size/rigidity of $Na^+$ channels and metal−ligand electrostatic interactions, how do other factors such as the filter's dielectric properties, oligomericity, and chemical composition, as well as the cation's coordination number (CN, number of metal-bound ligands) and HN, affect the $Na^+$ channel's selectivity? (2) In the epithelial $Na^+$ channel, do the serines lining the pore bind to the metal cation via their backbone or side chain O atoms? (3) In the voltage-gated $Na^+$ channel with the DEKA motif, how do the Lys protonation state and the Ala side chain orientation with respect to the pore lumen affect the channel's $Na^+/K^+$ selectivity? (4) How does the Lys in the DEKA motif play a pivotal role in selecting $Na^+$ over $K^+$? (5) Which of the two hypotheses—static or dynamic—is more plausible in explaining the mechanism of $Na^+/K^+$ selectivity in voltage-gated $Na^+$ channels?

This work addresses the above questions using density functional theory combined with continuum dielectric methods[34,62−65] to systematically evaluate the effect of various factors on the $Na^+$ vs $K^+$ selectivity in model $Na^+$ channel selectivity filters. These factors include (1) the HN and CN of the metal cation in the selectivity filter, (2) the number, chemical type, and charge of the coordinating groups lining the selectivity filter, and (3) the solvent exposure and the size/rigidity of the pore. $Na^+$ channel selectivity filters with metal coordinating groups differing in number (3 or 4) and type/charge [$-OH$, $-CONHCH_3$, $-COO^-$, $-NH_3^+$, $-NH(C{=}NH_2^+)NH_2$, and $-CH_3$] were modeled, as described in the next section. The first-shell ligands, which play a key role in the $Na^+/K^+$ competition, and the metal cations were treated explicitly using density functional theory to account for electronic effects such as polarization of the participating entities and charge transfer from the ligands to the metal cation, whereas the rest of the protein was represented by a continuum dielectric varying from 4 to 20 (see Methods). The findings of this work help delineate the key determinants of the $Na^+$ vs $K^+$ selectivity in $Na^+$ channels. By addressing the above questions, they also help to elucidate the metal-binding site structure in the selectivity filters of epithelial and voltage-gated $Na^+$ channels.

## Methods

**Models Used.** Models of trimeric and tetrameric $Na^+$ channel selectivity filters were built using GaussView version 3.09,[66] following the guidelines in our previous work.[34] The peptide backbone groups in the selectivity filters were modeled by $-CONHCH_3$, while the side chains of Ser, Asp/Glu, Lys, Arg, and Ala were modeled by $-OH$, $-COO^-$, $-NH_3^+$, $-NH(C{=}NH_2^+)NH_2$, and $-CH_3$, respectively. Different numbers of protein ligands were coordinated to the permeating ion ($Na^+$ or $K^+$), as observed experimentally,[10,15] and attached to a C−H ring scaffold via methylene spacers (see Figure 1).[34] In modeling the DEKA selectivity filter, the backbone amide group was additionally methylated to $-CON(CH_3)_2$ to avoid HN···COO hydrogen-bond formation with the neighboring carboxylate and distortion of the overall filter structure.

The structures modeling the selectivity filters were constructed on the basis of the following considerations:[34] (1) The ring mimics the oligomeric state of the ion channel protein, preventing the ligands from leaving the metal ion during geometry optimization. (2) The metal-ligating groups and their connection to the ring are flexible enough to allow them to optimize their positions upon metal binding. (3) The shape and C−H orientations of the ring do not obstruct the pore lumen. (4) As the number of carbon atoms in the trimeric ring (15 in Figure 1a,c,d) is similar to that in the tetrameric ring (16 in Figure 1b), the ring's C−H chain length would not bias the results.

**Metal Coordination and Hydration Numbers.** A recent Protein Data Bank[67] survey of $Na^+$ and $K^+$ binding sites in proteins shows that the metal CN ranges from 3 to 7 for $Na^+$ with a mean of ∼5 and from 4 to 9 for $K^+$ with a mean of ∼6.[68] Hence, in the model selectivity filters, metal CNs between 3 and 6 were considered. According to experimental observations, the number of first-shell water molecules bound to $Na^+$ is predominantly six, but varies from

(50) Noda, M.; Suzuki, H.; Numa, S.; Stuhmer, W. *FEBS Lett.* **1989**, *259*, 213–216.
(51) Terlau, H.; Heinemann, S. H.; Stuhmer, W.; Pusch, M.; Conti, F.; Imoto, K.; Numa, S. *FEBS Lett.* **1991**, *293*, 93–96.
(52) Pusch, M.; Noda, M.; Stuhmer, W.; Numa, S.; Conti, F. *Eur. Biophys. J.* **1991**, *20*, 127–133.
(53) Heinemann, S. H.; Terlau, H.; Stuhmer, W.; Imoto, K.; Numa, S. *Nature* **1992**, *356*, 441–443.
(54) Backx, P. H.; Yue, D. T.; Lawrence, J. H.; Marban, E.; Tomaselli, G. F. *Science* **1992**, *257*, 248–251.
(55) Favre, I.; Moczydlowski, E.; Schild, L. *Biophys. J.* **1996**, *71*, 3110–3125.
(56) Perez-Garcia, M.-T.; Chiamvimonvat, N.; Marban, E.; Tomaselli, G. F. *Proc. Natl. Acad. Sci. U.S.A.* **1996**, *93*, 300–304.
(57) Sun, Y. M.; Favre, I.; Schild, L.; Moczydlowski, E. *J. Gen. Physiol.* **1997**, *118*, 693–715.
(58) Hilber, K.; Sandtner, W.; Zarrabi, T.; Zebedin, E.; Kudlacek, O.; Fozzard, H. A.; Todt, H. *Biochemistry* **2005**, *44*, 13874–13882.
(59) Chiamvimonvat, N.; Perez-Garcia, M. T.; Ranjan, R.; Marban, E.; Tomaselli, G. F. *Neuron* **1996**, *16*, 1037–1047.
(60) Lipkind, G. M.; Fozzard, H. A. *Biochemistry* **2000**, *39*, 8161–8170.
(61) Lipkind, G. M.; Fozzard, H. A. *J. Gen. Physiol.* **2008**, *131*, 523–529.
(62) Dudev, T.; Lim, C. *Chem. Rev.* **2003**, *103*, 773–787.
(63) Dudev, T.; Lim, C. *J. Chin. Chem. Soc.* **2003**, *50*, 1093–1102.
(64) Dudev, T.; Lim, C. *Acc. Chem. Res.* **2007**, *40*, 85–93.
(65) Dudev, T.; Lim, C. *Annu. Rev. Biophys.* **2008**, *37*, 97–116.
(66) Gaussian, Pittsburgh, PA, 2000−2003.
(67) Berman, H. M.; et al. *Acta Crystallogr D* **2002**, *58*, 899–907.
(68) Noskov, S. Y.; Roux, B. *J. Mol. Biol.* **2008**, *377*, 804–818.

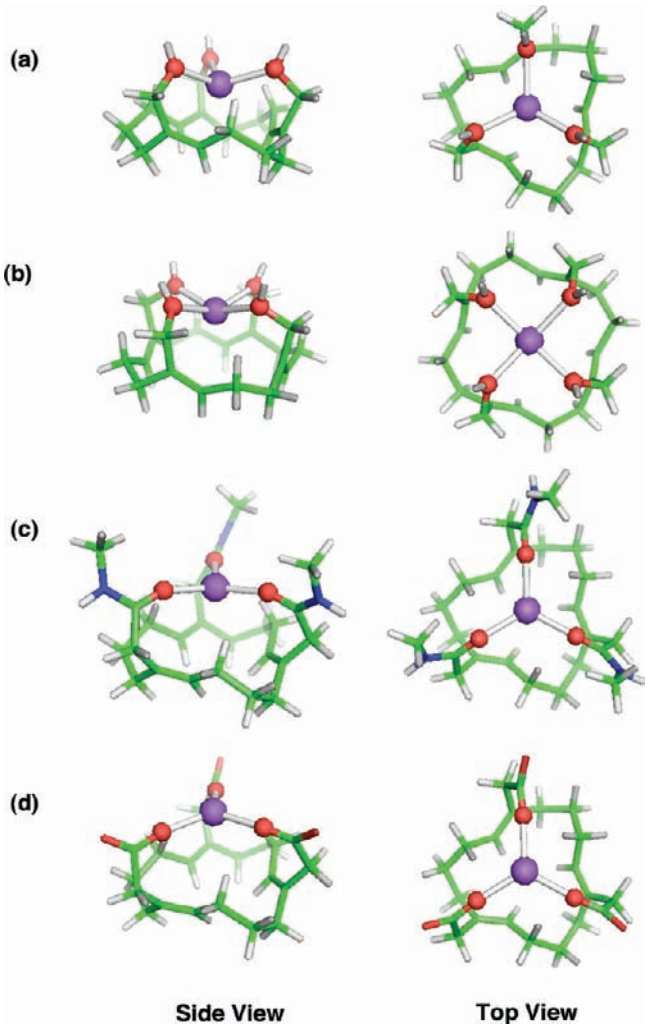


***Figure 1.*** Ball and stick diagrams of B3LYP/6-31+G(3d,p) fully optimized structures of $Na^+$ ligated to (a) three −OH groups of a trimeric filter, [filter3-$(OH)_3$], (b) four −OH groups of a tetrameric filter, [filter4-$(OH)_4$], (c) three −$CONHCH_3$ groups of a trimeric filter, [filter3-$(CONHCH_3)_3$], and (d) three −COO groups of a trimeric filter, [filter3-$(COO)_3$]. Color scheme: green, C; blue, N; red, O; gray, H; purple, Na.

six to eight for $K^+$ in aqueous solution.[69] In accord with the experimental findings, $Na^+$ hydrates were modeled as $[Na(H_2O)_6]^+$, while $K^+$ hydrates were modeled as $[K(H_2O)_6]^+$, $[K(H_2O)_7]^+$, and $[K(H_2O)_8]^+$.

**Reaction Modeled.** Sodium channel selectivity is an outcome of the competition between the bulk solvent and the protein ligands for the native $Na^+$ and a "rival" cation, e.g., $K^+$, and can be assessed by the free energy of the $K^+ \rightarrow Na^+$ exchange reaction,

$$[Na^+\text{-aq}] + [K^+\text{-filter}] \rightarrow [Na^+\text{-filter}] + [K^+\text{-aq}] \quad (1)$$

In eq 1, $[M^+\text{-aq}]$ and $[M^+\text{-filter}]$ ($M = Na^+$ or $K^+$) represent hydrated $Na^+$ or $K^+$ ions outside and bound inside the selectivity filter, respectively. The ion exchange free energy for eq 1 in a given environment characterized by a dielectric constant $\varepsilon = x$ is given by

$$\Delta G^x = \Delta G^1 + \Delta G^x_{solv}([Na^+\text{-filter}]) + \Delta G^x_{solv}([K^+\text{-aq}]) - \Delta G^x_{solv}([K^+\text{-filter}]) - \Delta G^x_{solv}([Na^+\text{-aq}]) \quad (2)$$

where $\Delta G^1$ is the gas-phase free energy and $\Delta G^x_{solv}$ is the free energy for transferring a molecule in the gas phase to a medium characterized by dielectric constant, $x$. The dielectric environment was assumed to be uniform for all participating entities, as the ion exchange was modeled to occur in the vicinity of the selectivity filter. Since previous studies[31,33] showed that the ion channel selectivity filter and its immediate surroundings are *not* in a bulk water environment ($\varepsilon \neq 80$), a dielectric constant $\varepsilon = 4$, 10, or 20, mimicking binding sites of increasing solvent exposure, was used.

**Gas-Phase Free Energy Calculations.** Among several combinations of different ab initio/density functional methods (HF, MP2, S-VWN, B3-LYP) and basis sets [6-31+G(d,p), 6-31+G(2d,2p), 6-31+G(3d,p), 6-31+G(3d,2p), 6-311++G(d,p), 6-311++G-(3df,3pd)], the B3-LYP/6-31+G(3d,p) method was found to be the most efficient in yielding dipole moments of the metal ligands that are closest to the respective experimental values and to reproduce (within experimental error) the Na/K−O distances in crown-ether complexes, which resemble metal-occupied ion channel pores.[34] Hence, it was used to optimize the geometry of each metal complex without any constraints and to compute the electronic energies, $E_{el}$, using the Gaussian 03 program.[70] However, the smaller 6-31+G(d,p) basis set was used to compute the vibrational frequencies for the respective complexes due to computer memory limitations. No imaginary frequency was found in any of the complexes. The B3-LYP/6-31+G(d,p) frequencies were scaled by an empirical factor of 0.9613[71] and used to compute the thermal energies including zero-point energy ($E_{th}$) and entropies ($S$) from standard statistical mechanical formulas.[72] Using the scaled 6-31+G(d,p) frequencies instead of the scaled 6-31+G(3d,p) frequencies has been shown to result in little change (<0.2 kcal/mol) in the $\Delta E_{th}$ and $\Delta S$ differences between Na- and K-occupied trimeric selectivity filter models.[34]

The differences in $\Delta E_{el}$, $\Delta E_{th}$, $\Delta PV$ (work term), and $\Delta S$ between the products and reactants in eq 1 were used to calculate $\Delta G^1(K^+ \rightarrow Na^+)$ in the gas phase at $T = 298.15$ K according to

$$\Delta G^1 = \Delta E_{el} + \Delta E_{th} + \Delta PV - T\Delta S \quad (3)$$

Since the basis set superposition error was found to be negligible for the ion exchange reactions (eq 1) in previous work,[34] it was not considered in the present calculations.

**Solution Free Energy Calculations.** The $\Delta G^x_{solv}$ were estimated by solving Poisson's equation using finite difference methods[73,74] with the MEAD (Macroscopic Electrostatics with Atomic Detail) program,[75] as described in previous works.[76] The effective solute radii were obtained by adjusting the CHARMM (version 22)[77] van der Waals radii to reproduce the experimental hydration free energies of $Na^+$, $K^+$, and model ligand molecules to within 1 kcal/mol.[34] The resulting values (in Å) are $R_{Na} = 1.72$, $R_K = 1.90$, $R_C = 1.95$, $R_N = 1.75$, $R_O(-CONHCH_3) = 1.72$, $R_O(H_2O) = 1.85$, $R_O(-CH_2OH) = 1.90$, $R_O(-COO^-) = 1.56$, $R_H = 1.50$, $R_H(H_2O-Na) = 1.26$, $R_H(H_2O-K) = 1.20$. Natural bond orbital atomic charges, which are known to be numerically stable with respect to basis set changes,[78] were used to compute $\Delta G^x_{solv}$. Changing the population analysis method does not significantly change the difference in solvation free energies between the

(69) Marcus, Y. *Chem. Rev.* **1988**, *88*, 1475–1498.
(70) Frisch, M. J. Gaussian, Inc.: Pittsburgh, PA, 2003.
(71) Wong, M. W. *Chem. Phys. Lett.* **1996**, *256*, 391–399.
(72) McQuarrie, D. A. *Statistical Mechanics*; Harper and Row: New York, 1976.
(73) Gilson, M. K.; Honig, B. *Proteins: Struct. Func. Genet.* **1988**, *4*, 7–18.
(74) Lim, C.; Bashford, D.; Karplus, M. *J. Phys. Chem.* **1991**, *95*, 5610–5620.
(75) Bashford, D. In *Scientific Computing in Object-Oriented Parallel Environments*; Ishikawa, Y., Oldehoeft, R. R., Reynders, V. W., Tholburn, M., Eds.; Springer: Berlin, 1997; Vol. 1343, pp 233−240.
(76) Dudev, T.; Lim, C. *J. Am. Chem. Soc.* **2006**, *128*, 1553–1561.
(77) Brooks, B. R.; Bruccoleri, R. E.; Olafson, B. D.; States, D. J.; Swaminathan, S.; Karplus, M. *J. Comput. Chem.* **1983**, *4*, 187–217.
(78) Reed, A. E.; Curtiss, L. A.; Weinhold, F. *Chem. Rev.* **1988**, *88*, 899–926.

***Table 1.*** Calculated Electronic Energies, Entropies, and Free Energies (in kcal/mol) of Ion Selectivity for Rigid Hydroxyl-Containing Selectivity Filters in Media of Varying Dielectric Constant

| | reaction[a] | $\Delta E_{el}$ | $T\Delta S^1$ | $\Delta G^1$ | $\Delta G^4$ | $\Delta G^{10}$ | $\Delta G^{20}$ |
|---|---|---|---|---|---|---|---|
| 1 | $[NaW_6]^+ + [K\text{-filter3-}(OH)_3]^+ \rightarrow [Na\text{-filter3-}(OH)_3]^+ + [KW_6]^+$ | −2.0 | −0.8 | −0.8 | −0.4 | −0.6 | −0.7 |
| 2 | $[NaW_6]^+ + [K\text{-filter3-}(OH)_3]^+ + W \rightarrow [Na\text{-filter3-}(OH)_3]^+ + [KW_7]^+$ | −14.2 | −10.3 | −1.9 | 3.0 | 4.2 | 4.6 |
| 3 | $[NaW_6]^+ + [K\text{-filter3-}(OH)_3]^+ + 2W \rightarrow [Na\text{-filter3-}(OH)_3]^+ + [KW_8]^+$ | −26.0 | −19.4 | −3.2 | 6.6 | 9.7 | 11.0 |
| 4 | $[NaW_6]^+ + [K\text{-filter4-}(OH)_4]^+ \rightarrow [Na\text{-filter4-}(OH)_4]^+ + [KW_6]^+$ | −0.3 | −2.3 | 2.5 | 2.3 | 1.9 | 1.7 |
| 5 | $[NaW_6]^+ + [K\text{-filter4-}(OH)_4]^+ + W \rightarrow [Na\text{-filter4-}(OH)_4]^+ + [KW_7]^+$ | −12.5 | −11.9 | 1.4 | 5.7 | 6.7 | 7.0 |
| 6 | $[NaW_6]^+ + [K\text{-filter4-}(OH)_4]^+ + 2W \rightarrow [Na\text{-filter4-}(OH)_4]^+ + [KW_8]^+$ | −24.3 | −20.9 | 0.1 | 9.3 | 12.2 | 13.4 |

[a] W denotes a water molecule. For the reverse reactions, the released water molecule(s) are assumed to be in the vicinity of the selectivity filter, characterized by a dielectric constant $x$ (see the text). The computed solvation free energy $\Delta G^x_{solv}$ for the free water molecule (in kcal/mol) is −3.9 for $x = 4$, −5.4 for $x = 10$, −6.1 for $x = 20$, and −6.7 for $x = 80$. Note that the latter is in close agreement with the respective experimental hydration free energy (−6.3 kcal/mol).

respective counterparts in the metal selectivity process (eq 1). For example, $\Delta G^{10}_{solv}$[Na-filter3-(OH)$_3$] − $\Delta G^{10}_{solv}$[K-filter3-(OH)$_3$] is 1.3 kcal/mol with natural bond orbital atomic charges and 1.0 kcal/mol with CHelpG and Merz−Kollman charges.

## Results

**Selectivity Filters Lined with Hydroxyl Groups.** Table 1 lists the free energies for replacing $K^+$ with $Na^+$ in tri- and tetrameric filters lined with three or four hydroxyl groups of varying degrees of solvent exposure. The computed free energy differences, $\Delta G^x$ ($x = 4$, 10, 20), should be considered to be qualitative rather than quantitative, as they were estimated using B3-LYP/6-31+G(3d,p) gas-phase free energies combined with an implicit solvent model. Nevertheless, they can reproduce the trend in ion selectivity of 18-crown-6 ether in aqueous solution, as shown in our previous work:[34] The computed $\Delta G(K^+ \rightarrow Na^+)$ for $[Na(H_2O)_6]^+ + [K(18\text{-crown-6})]^+ \rightarrow [Na(18\text{-crown-6})]^+ + [K(H_2O)_6]^+$ (1.4 kcal/mol) is in accord with the experimental value (2.0 ± 0.1 kcal/mol).[79] Hence, their trends should be reliable.

**Dependence on the $K^+$ Hydration Number.** To evaluate the effect of the $K^+$ HN in determining the pore's ion selectivity, $K^+ \rightarrow Na^+$ exchange free energies were computed with $K^+$ bound to six, seven, or eight water molecules, in line with experimental observations. In the gas phase, increasing the HN of $K^+$ relative to that of $Na^+$ favors $Na^+$ over $K^+$ in trimeric selectivity filters lined with three hydroxyl groups. For the first three reactions in Table 1, increasing the $K^+$ HN from 6 to 8 decreases $\Delta E_{el}$ (from −2.0 to −26.0 kcal/mol) more than $T\Delta S^1$ (from −0.8 to −19.4 kcal/mol); thus, the resultant $\Delta G^1$ also decreases slightly (from −0.8 to −3.2 kcal/mol). This implies that in the absence of a protein matrix, increasing the HN of $K^+$ relative to that of $Na^+$ favors $Na^+$ over $K^+$ in trimeric selectivity filters, as the enthalpic gain upon binding extra water molecule(s) to $K^+$ outweighs the respective entropic loss of orienting the water O toward $K^+$.

The trend observed in the gas phase, however, is reversed in the presence of the protein solution environment. Comparison of the $\Delta G^x$ ($x = 4$, 10, 20) free energies for each triad of reactions in Table 1 shows that in both trimeric and tetrameric selectivity filters, increasing the HN of $K^+$ relative to that of $Na^+$ favors $K^+$ over $Na^+$ (more positive $\Delta G^x$); e.g., the $\Delta G^4$ for reactions 1, 2, and 3 are −0.4, 3.0, and 6.6 kcal/mol, respectively. This is mainly because when $K^+$ replaces $Na^+$ in the filter with the same CN (reverse of the reactions in Table 1), water molecules are released and become favorably solvated if the HN of $K^+$ exceeds that of $Na^+$. These results suggest that a protein matrix that favors a *lower* $K^+$ HN inside the pore would help to select $Na^+$ over $K^+$.

**Dependence on the Filter's Solvent Exposure.** Previous work[31] showed that the dielectric constant is inversely correlated with the $K^+$ HN: Metal-binding sites with *higher* solvent accessibility (higher dielectric constant) favor a *lower* $K^+$ HN, which in turn would favor $Na^+$ binding (see above). Indeed, the results in Table 1 show that increasing the filter's solvent exposure (dielectric constant $x$), which yields a lower $K^+$ HN, reduces $K^+/Na^+$ selectivity or favors $Na^+$ over $K^+$. As $x$ increases in the trimeric selectivity filter, the $\Delta G^x$ becomes more favorable and decreases from 6.6 kcal/mol for reaction 3 involving octahydrated $K^+$ when $x = 4$ to −0.7 kcal/mol for reaction 1 involving hexahydrated $K^+$ when $x = 20$.

**Dependence on the Filter's Hydroxyl Group Number.** To evaluate the effect of the *number* of coordinating dipoles lining

(79) Ozutsumi, K.; Ishigiro, S. *Bull. Chem. Soc. Jpn.* **1992**, *65*, 1173–1175.

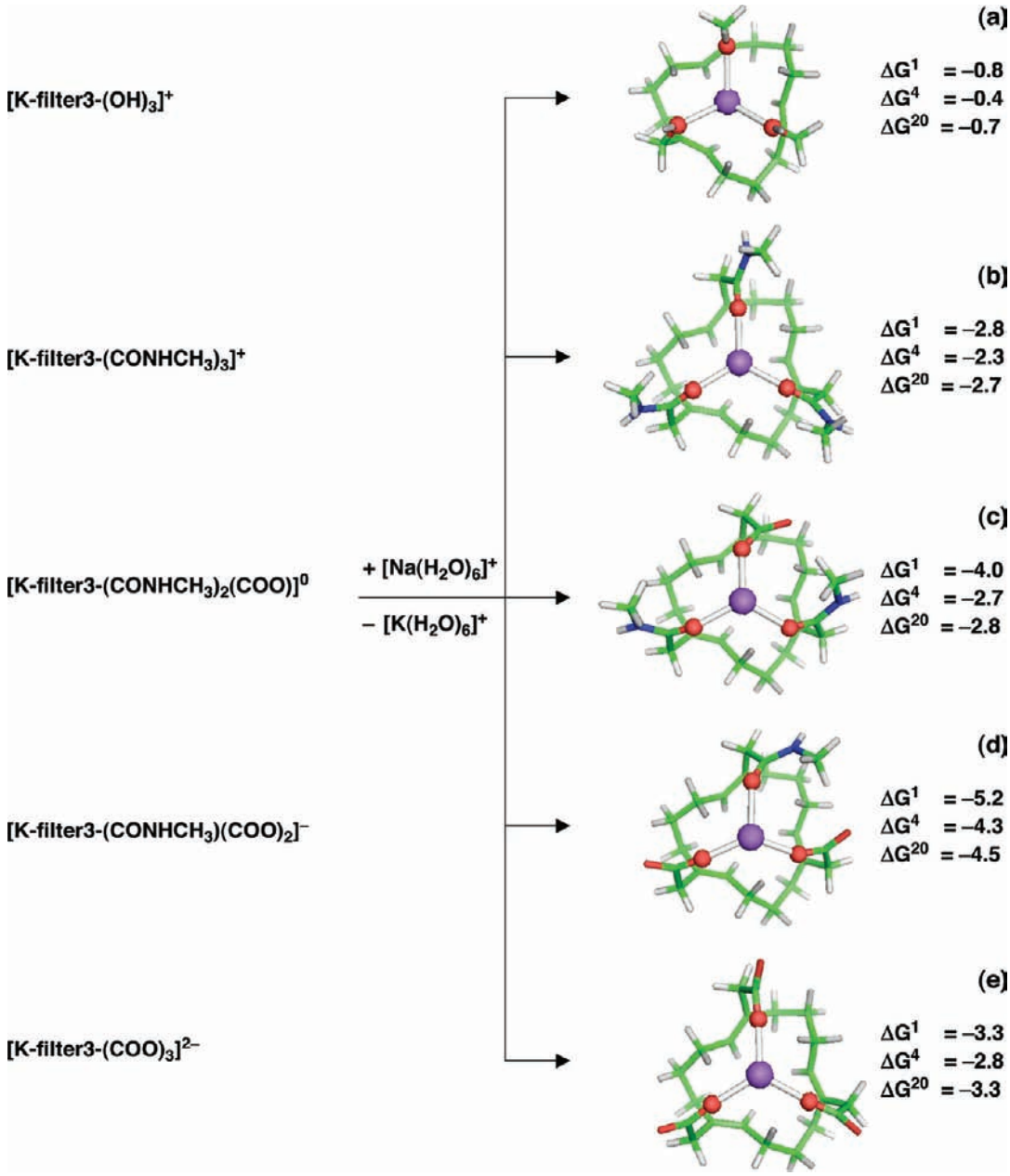


***Figure 2.*** Free energies (in kcal/mol) for replacing fully dehydrated $K^+$ with $Na^+$ in trimeric filters containing ligands of increasing ligating strength. (a) [filter3-$(OH)_3$], (b) [filter3-$(CONHCH_3)_3$], (c) [filter3-$(CONHCH_3)_2(COO)$], (d) [filter3-$(CONHCH_3)(COO)_2$], and (e) [filter3-$(COO)_3$]. Color scheme: green, C; blue, N; red, O; gray, H; purple, Na.

the pore in determining its ion selectivity, $K^+ \rightarrow Na^+$ exchange free energies $\Delta G^x$ were computed with the dehydrated ion bound to three or four OH groups. Comparison of the $\Delta G^x$ in trimeric (reactions 1−3) and tetrameric filters (reactions 4−6) shows that decreasing the number of coordinating dipoles is favorable for $Na^+$ binding: the $\Delta G^x$ ($x = 4-20$) values for the trimeric filter are negative or less positive than $\Delta G^x$ of its tetrameric counterpart. For example, in Table 1, $\Delta G^4/\Delta G^{20}$ for the trimeric filter (−0.4/−0.7 kcal/mol, reaction 1) is more favorable than that for the tetrameric pore (2.3/1.7 kcal/mol, reaction 4). These results reflect the stronger dislike of the small $Na^+$ for a crowded coordination sphere, where unfavorable dipole−dipole repulsion and "freezing" of dipole orientations outweigh favorable metal−ligand interactions.[34]

In summary, the above findings indicate that a selectivity filter that is relatively rigid (forcing $K^+$ to adopt the same CN as $Na^+$), solvent exposed (thus favoring hexahydrated $Na^+$ and $K^+$ cations), and lined with three hydroxyl metal-ligating groups would be selective for $Na^+$. This is consistent with a recent survey[68] showing that in protein structures, binding sites containing $Na^+$ bound to neutral ligands are frequently located at the protein surface and are lined by three protein ligands.

**Selectivity Filters Lined with Carbonyl and Carboxyl Groups.** In the epithelial $Na^+$ channel, the serines lining the selectivity filter can bind to $Na^+/K^+$ via their backbone or side chain O atoms, which differ in polarizability and the absolute dipole moment. In voltage-gated $Na^+$ channels, the four highly conserved DEKA residues lining the selectivity filter can bind to $Na^+/K^+$ via the carboxylate and/or carbonyl O atoms, which differ in charge. Below, we address how the different charge-donating ability and thus different ligating strengths of these coordinating groups affect $Na^+/K^+$ selectivity.

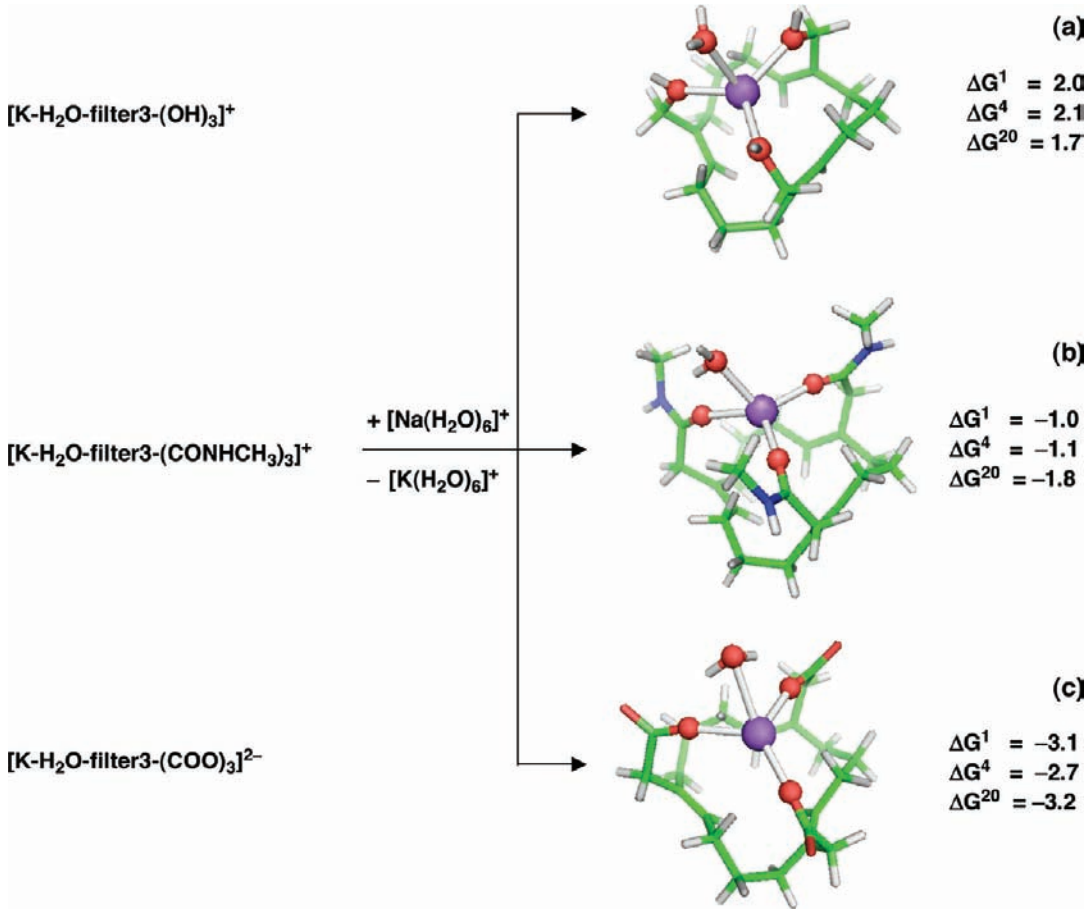


***Figure 3.*** Free energies (in kcal/mol) for replacing partially hydrated $K^+$ with $Na^+$ in trimeric filters containing ligands of increasing ligating strength. (a) [filter3-$(OH)_3$], (b) [filter3-$(CONHCH_3)_3$], and (c) [filter3-$(COO)_3$]. Color scheme: green, C; blue, N; red, O; gray, H; purple, Na.

**Dependence on the Ligating Strength of the Protein Ligands.** This was assessed by computing the $K^+ \rightarrow Na^+$ exchange free energies, $\Delta G^x$ ($x = 1-20$), in trimeric filters lined with different coordinating groups ($-OH$, $-CONHCH_3$, and $-COO^-$). The results show that increasing the ligating strength of the protein ligand enhances $Na^+/K^+$ selectivity. Between the two neutral groups, the carbonyl group has a larger dipole moment and stronger charge-donating ability than the hydroxyl group;[20,65] thus, selectivity filters lined with three $-CONHCH_3$ (Figure 2b) are more selective for $Na^+$ than those lined with three $-OH$ groups (Figure 2a): the $\Delta G^x$ for replacing $K^+$ with $Na^+$ in the former are more negative than those for the latter. The above observation is in accord with the classical field strength concepts introduced by Eisenman,[20] predicting that a ligand with a higher field strength (carbonyl in this case) would favor $Na^+$ over $K^+$.

Substituting one or two carbonyl groups in filter3-$(CONHCH_3)_3$ (Figure 2b) for carboxylates with even higher ligating strength (Figure 2c,d) results in more favorable $K^+ \rightarrow Na^+$ exchange free energies; e.g., $\Delta G^4$ decreases from $-2.3$ kcal/mol in Figure 2b to $-2.7$ kcal/mol in Figure 2c and $-4.3$ kcal/mol in Figure 2d. Introducing a third carboxylate ligand (Figure 2e), however, does not lead to further decrease in the ion exchange free energy. Instead, although the free energies for the reaction in Figure 2e are still negative, they are less favorable than those for the preceding reaction in Figure 2d. This decline in the free energy magnitude for filter3-$(COO^-)_3$ is probably because the repulsion among the three anionic ligands surrounding $Na^+$ is greater than that surrounding the larger $K^+$ ($\Delta G^1$ in Figure 2e is less negative than $\Delta G^1$ in Figure 2c or Figure 2d).

**Dependence on the Metal's Partial Hydration and Its Coordination Number in the Filter.** To assess the effect of the metal's partial hydration inside the filter and corresponding variations in its CN on the $Na^+/K^+$ selectivity, the free energies of $K^+ \rightarrow Na^+$ exchange in trimeric filters with the metal cation coordinated to three $-OH$, three $-CONHCH_3$, or three $-COO^-$ groups and a water molecule were evaluated (Figure 3). Partial hydration of the metal ion, which increases its CN from 3 to 4, decreases the $Na^+/K^+$ selectivity in trimeric filters lined with neutral ligating groups: the $\Delta G^x$ values in parts a and b of Figure 3 are less favorable than those in parts a and b of Figure 2, respectively. This is consistent with the above finding that increasing the number of metal-coordinating dipoles disfavors $Na^+$ selectivity (Table 1).

The negative effect of partial metal hydration on $Na^+/K^+$ selectivity for the three types of selectivity filters in Figure 3 appears to be inversely correlated with the ligating strength of the pore-lining groups: The effect is more pronounced for trimeric filters with weak-ligating OH groups, as opposed to stronger-ligating $CONHCH_3$ groups: the $\Delta G^4/\Delta G^{20}$ values in parts a and b of Figure 3 increase by $\sim$2.5 and $\sim$1 kcal/mol relative to those in parts a and b of Figure 2, respectively. With even stronger-ligating moieties such as $COO^-$ groups, retaining a metal-bound water molecule has negligible effect on the selectivity of the trimeric filter: the $\Delta G^4/\Delta G^{20}$ values in Figures

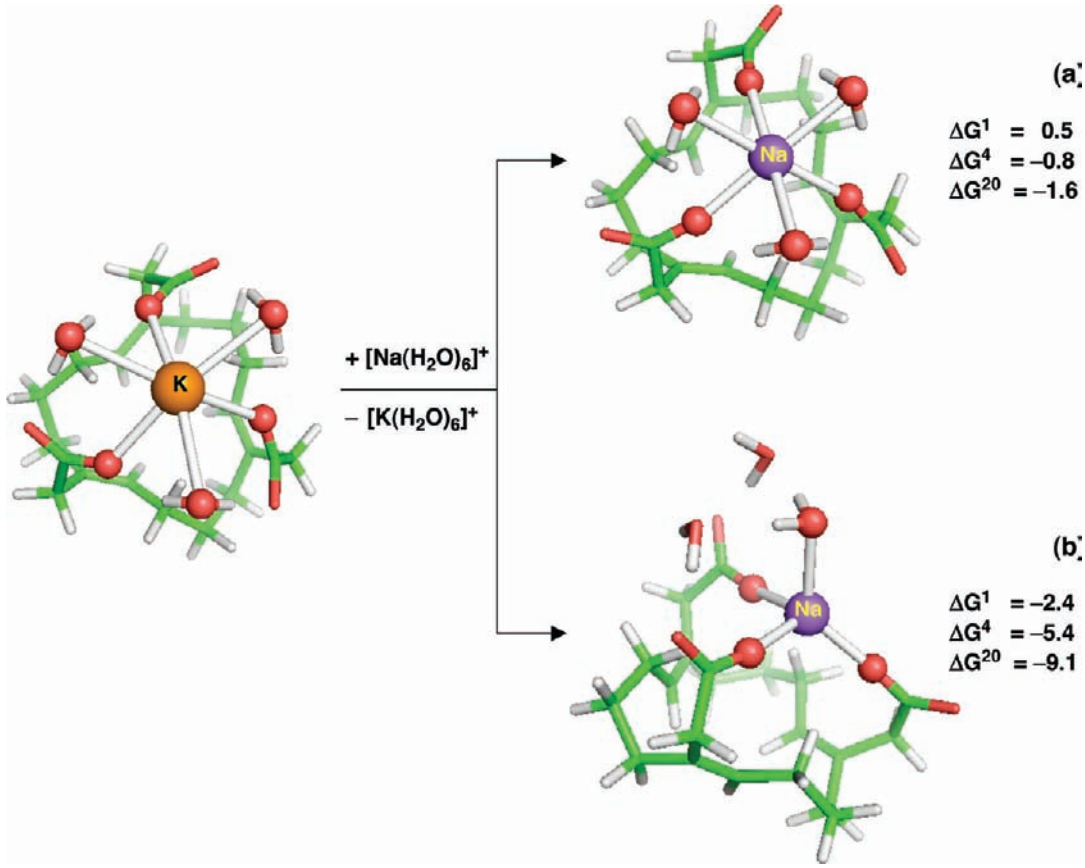


***Figure 4.*** Free energies (in kcal/mol) for replacing $K^+$ in [$(H_2O)_3$-filter3-$(COO)_3$] with $Na^+$ (a) hexacoordinated to three carboxylates and three water molecules, and (b) tetracoordinated directly to three carboxylates and one water molecule and indirectly to two water molecules in the second coordination layer. Color scheme: green, C; blue, N; red, O; gray, H; purple, Na; orange, K.

3c and 2e differ by only 0.1 kcal/mol. This is because the relative contribution of the water molecule in forming the partially hydrated complexes decreases with increasing the dipole moment/charge of the pore-lining groups. For example, the water (W) contribution to the formation energy of [Na-W-filter3-$(OH)_3]^+$ is 8.5%, and decreases to 7.4% in [Na-W-filter3-$(CONHCH_3)_3]^+$ and 4.7% in [Na-W-filter3-$(COO)_3]^{2-}$.

Increasing the metal CN by retaining more metal-bound water molecules further compromises the $Na^+$ selectivity of the pore. In complexes where both $K^+$ and $Na^+$ are hexacoordinated and bound to a trimeric tricarboxylate filter and three water molecules (Figure 4a), the $\Delta G^4/\Delta G^{20}$ for $K^+ \rightarrow Na^+$ exchange decreases in absolute value by ~2 kcal/mol relative to the water-free filter (Figure 2e). However, if the pore allows $Na^+$ to adopt a smaller CN than $K^+$, the filter's selectivity for $Na^+$ increases. Substituting a hexacoordinated $K^+$ by a tetracoordinated $Na^+$ (with two water molecules in the second layer) favors $Na^+$ selectivity ($\Delta G^4/\Delta G^{20}$ in Figure 4b is more negative than that in Figure 4a). In general, decreasing the CN of a given metal relative to that of its competitor favors the cation with the smaller CN (see Supporting Information).

**Dependence on the Pore's Size/Rigidity.** To establish to what extent the pore's size/rigidity affects the selectivity process, the energies of rigid $Na^+$-optimized pores, where the "native" $Na^+$ was substituted for $K^+$, were evaluated. Specifically, $Na^+$ from the fully optimized metal-bound trimeric filters, [Na-filter3-$(OH)_3]^+$ (Figure 1a) and [Na-filter3-$(CONHCH_3)_3]^+$ (Figure 1c), was replaced by $K^+$ and the resultant structures, without reoptimization, were subjected to single-point calculations at the B3-LYP/6-31+G(3d,p) level. These calculations mimic $K^+$ binding to rigid narrow pores that are optimal for $Na^+$. Their purpose is to yield trends of changes rather than quantitative results, as absolutely rigid pores, as modeled here, are unlikely due to thermal motion of the atoms. They show that forcing $K^+$ into a constricted pore, designed to fit $Na^+$, is energetically unfavorable, due to an elevated electronic energy for the respective $K^+$-bound pores. Relative to the gas-phase $\Delta E_{el}$ energy in Table 1, the $\Delta E_{el}$ for replacing $K^+$ with $Na^+$ in filter3-$(OH)_3$ and in filter3-$(CONHCH_3)_3$ decreases (by 19.0 and 23.6 kcal/mol, respectively), which increases the filter's selectivity for $Na^+$ (more negative values for the respective free energies). These energy changes appear to be inversely correlated with the pore's radius, $R_{pore}$, which in the case of a symmetric trimeric filter is determined by the ion−O distance. The pore size, in turn, is correlated with the pore's relative rigidity, as reflected by the gas-phase entropic change. Hence, the [Na-filter3-$(CONHCH_3)_3]^+$ filter with a narrow and rigid pore ($R_{pore} = 2.22$ Å; $\Delta S = 0.1$ cal/mol K) is more selective than the [Na-filter3-$(OH)_3]^+$ filter, which has a larger and more flexible pore ($R_{pore} = 2.32$ Å; $\Delta S = 3.6$ cal/mol K).

Notably, the energy cost for replacing the native $Na^+$ with a bulkier $K^+$ in a narrow pore optimized for $Na^+$ (19−24 kcal /mol) is almost twice that for replacing the native $K^+$ with a smaller $Na^+$ in a wider pore optimized for $K^+$, viz., the fully optimized tetrameric K-filter4-$(CONHCH_3)_4$ whose $R_{pore} = 2.65$ Å. These results imply that the pore's size/rigidity plays a more important role in determining the $Na^+/K^+$ selectivity in $Na^+$-optimized filters than the $K^+/Na^+$ selectivity in the corresponding

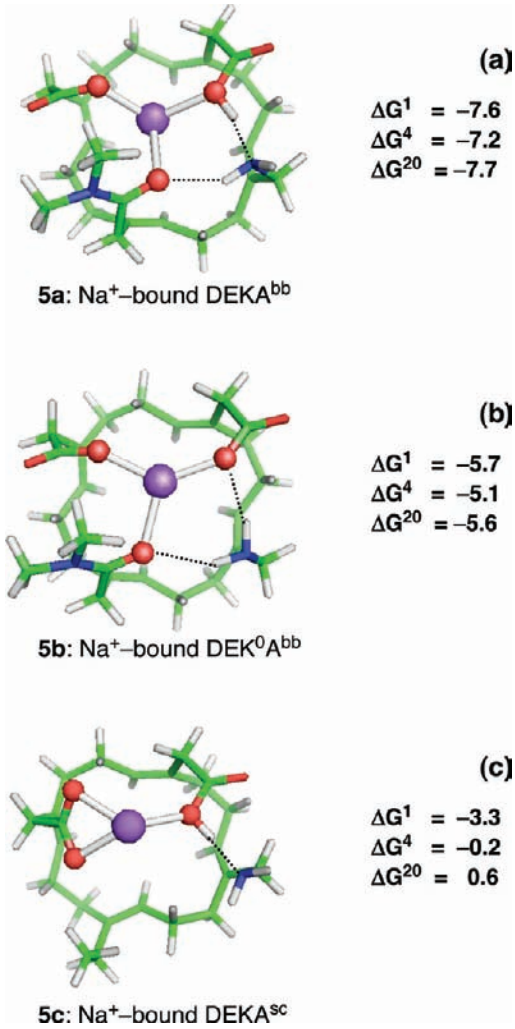


***Figure 5.*** Models of voltage-gated Na channels with a DEKA filter: (a) [Na-filter4-$(COO)_2(NH_3^+)(CON(CH_3)_2)$]$^0$ modeling $Na^+$-bound $DEKA^{bb}$ filter (**5a**), (b) [Na-filter4-$(COO)_2(NH_2)(CON(CH_3)_2)$]$^-$ mimicking $Na^+$-bound $DEK^0A^{bb}$ filter (**5b**), and (c) [Na-filter4-$(COO)_2(NH_3^+)(CH_3)$]$^0$ modeling $Na^+$-bound $DEKA^{sc}$ filter (**5c**), where the $K^0$ denotes deprotonated Lys, while $A^{bb}$ and $A^{sc}$ denote the Ala backbone and side chain facing the pore lumen, respectively. The fully optimized B3LYP/6-31+G(3d,p) structures are depicted on the left, while the free energies for $[NaW_6]^+ + [K^+\text{-filter4}] \rightarrow [Na^+\text{-filter4}] + [KW_6]^+$ (in kcal/mol) are shown on the right. Color scheme: green, C; blue, N; red, O; gray, H; purple, Na.

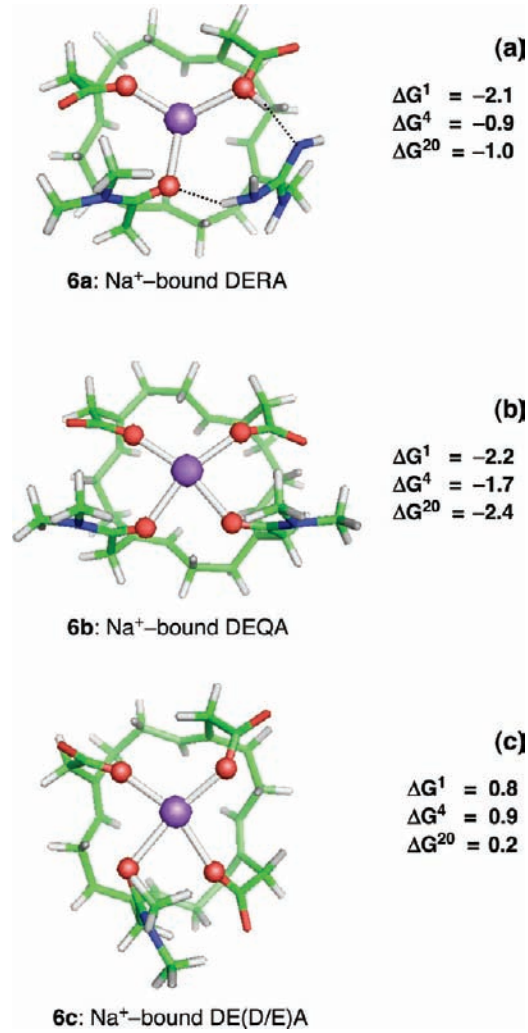


***Figure 6.*** Models of voltage-gated Na channels where the Lys side chain comprising the DEKA motif has been mutated to (a) $-NH(C{=}NH_2^+)NH_2$, mimicking the Arg side chain in the $Na^+$-bound DE**R**A filter (**6a**), (b) $-CON(CH_3)_2$, mimicking the backbone amide group in the $Na^+$-bound DE**Q**A filter (**6b**), and (c) $-COO^-$, mimicking the Asp/Glu side chain in the $Na^+$-bound DE(**D/E**)A filter (**6c**). The fully optimized B3LYP/6-31+G(3d,p) structures are depicted on the left, while the free energies for $[NaW_6]^+ + [K^+\text{-filter4}] \rightarrow [Na^+\text{-filter4}] + [KW_6]^+$ (in kcal/mol) are shown on the right. Color scheme: green, C; blue, N; red, O; gray, H; purple, Na.

$K^+$-optimized structures. This is in accord with previous findings that the pore's size/rigidity plays a more important role in determining the $Na^+$ vs $K^+$ selectivity in $Na^+$ channels,[55,57,58,68,80] than in determining the $K^+$ vs $Na^+$ selectivity in $K^+$ channels.

**Selectivity Filters with the DEKA Motif.** To see how the above findings help in understanding the mechanism of metal selectivity in tetrameric voltage-gated $Na^+$ channels with a DEKA selectivity filter, we studied the $Na^+/K^+$ competition in several tetrameric filters lined with metal-coordinating groups modeling the Asp/Glu, Lys, and Ala side chains and peptide backbone group. The lack of 3D structures of voltage-gated $Na^+$ channels with a DEKA selectivity filter leaves open questions about (a) the Lys protonation state, (b) the Ala side chain orientation, (c) why the mutation of Lys to another aa residue drastically reduces or even reverses the $Na^+/K^+$ selectivity, and (d) whether the static or dynamic hypothesis is more plausible in explaining the mechanism of $Na^+/K^+$ selectivity in voltage-gated $Na^+$ channels.

**Wild-Type Filter.** To evaluate the binding mode of the DEKA residues to $Na^+$ or $K^+$, we explored various possible structures of these pores where (1) the Ala backbone carbonyl group[60,61] (Figure 5a,b) or its side chain methyl group[59] (Figure 5c) faces the pore lumen and (2) the Lys side chain is protonated (Figure 5a,c) or deprotonated (Figure 5b). Notably, when the Lys is protonated, a proton from $-NH_3^+$ is transferred to the adjacent carboxylate during optimization of the Na-/K-bound structure. The fully optimized structures in Figure 5 show that although the DEKA filter has a tetrameric structure, the metal cation binds to only three protein ligand atoms: $Na^+$ is bound monodentately to the Asp and Glu carboxylate O and the Ala carbonyl O (Figure 5a,b) or monodentately to one carboxylate and bidentately to the other carboxylate if the Ala backbone is not oriented toward the pore (Figure 5c).

(80) Boda, D.; Nonner, W.; Valisko, M.; Henderson, D.; Eisenberg, B.; Gillespie, D. *Biophys. J.* **2007**, *93*, 1960–1980.

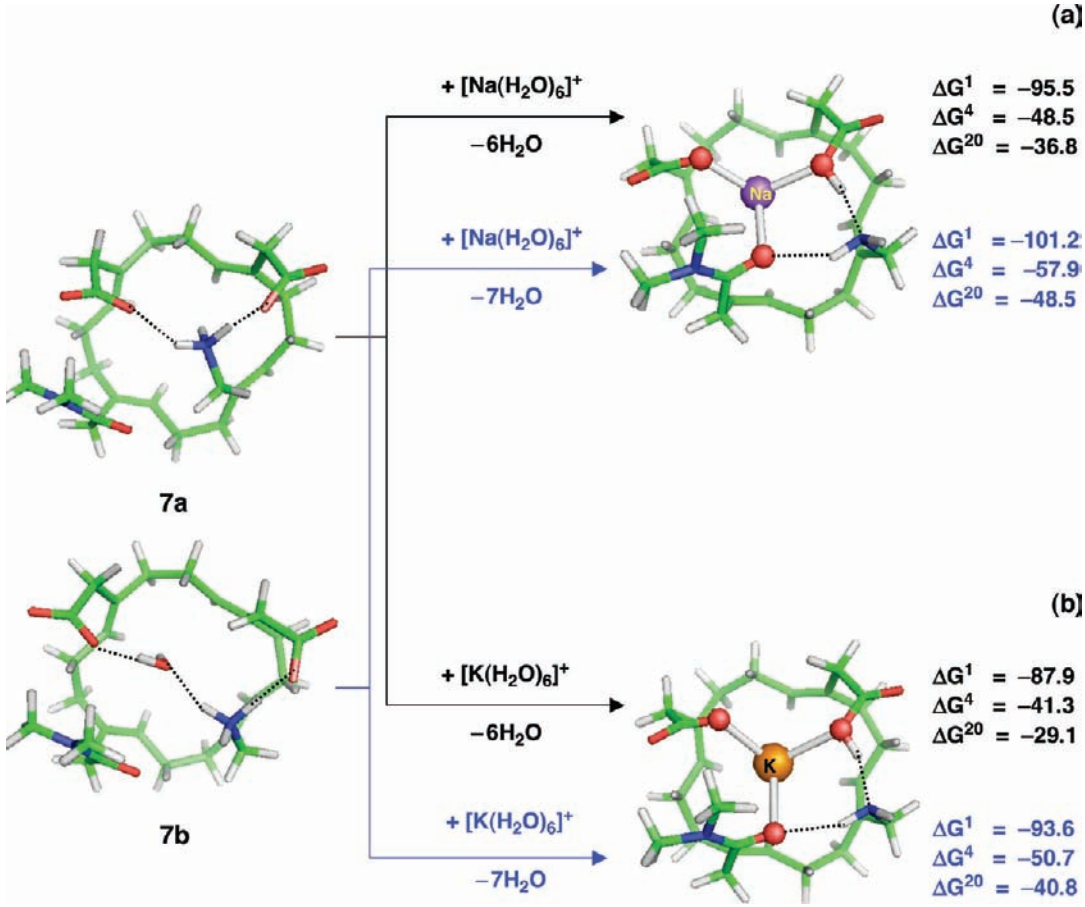


***Figure 7.*** Free energies (in kcal/mol) for (a) $Na^+$ and (b) $K^+$ binding to tetrameric filters with the DEKA locus. Reactions in black refer to a fully dehydrated pore (**7a**), while reactions in blue refer to a pore with a water molecule bridging the Lys and Asp residues (**7b**). Color scheme: green, C; blue, N; red, O; gray, H; purple, Na; orange, K.

The Lys side chain (protonated or deprotonated) does not bind directly to the metal ion but hydrogen bonds to the neighboring carboxylate and carbonyl groups, thus rigidifying/constricting the pore aperture, contributing to the $Na^+$ vs $K^+$ selectivity in voltage-gated $Na^+$ channels. This effect appears to be more pronounced in structure **5a** with protonated Lys than in the alternative structure **5b** with neutral Lys: The triangular pore in **5a** (whose size is estimated by the sum of the distances between the three metal-bound O atoms, $\sum = 10.6$ Å, and the area of the triangle, $\sigma = 5.4$ Å$^2$) is narrower than that in **5b** (where $\sum = 11.3$ Å and $\sigma = 6.0$ Å$^2$), yielding more favorable $K^+ \rightarrow Na^+$ exchange free energies for the former than the latter. Thus, the filter with protonated Lys appears to be more selective for $Na^+$ than the respective structure with deprotonated Lys. However, both filters are well suited to select $Na^+$ over $K^+$.

The Ala backbone also contributes to the $Na^+/K^+$ selectivity in $Na^+$ channels with a DEKA pore, as its carbonyl O can bind to the metal ion and interact with the neighboring Lys. This is evidenced by the fact that when the Ala backbone amide is replaced by the inert $-CH_3$ (modeling the Ala side chain, Figure 5c), the hydrogen bond with the Lys side chain is lost, and the neighboring carboxylate becomes bidentately bound to the metal ion. The $Na^+/K^+$ selectivity is almost abolished in **5c**, indicating that the DEKA filter with the Ala backbone facing the pore lumen is more selective for $Na^+$ than that with the Ala side chain pointing into the pore.

**Mutant Structures.** Among the four residues comprising the DEKA motif, Lys is the critical determinant that specifies the selective permeability of $Na^+$ over $K^+$ in voltage-gated $Na^+$ channels: mutating this Lys to any other residue greatly reduces or abolishes or even reverses the pore's selectivity for $Na^+$.[7,55,57,58] For example, mutating the DE**K**A lysine to a neutral residue (Gln) greatly reduces the $Na^+$ selectivity: the permeability ratio, $P_{K^+}/P_{Na^+}$, increases from 0.10 ± 0.03 for the DE**K**A filter in rat brain $Na^+$ channel to 0.76 ± 0.06 for DE**Q**A.[7] Substituting the DEKA lysine with another positively charged residue, Arg, almost abolishes the channel's selectivity for $Na^+$, whereas mutating it to a negatively charged residue such as Cys reverses the channel's selectivity: the $P_{K^+}/P_{Na^+}$ increases from 0.03 ± 0.01 for the DE**K**A filter in rat muscle $Na^+$ channel to 0.90 ± 0.04 for the DE**R**A mutant and to 1.20 ± 0.07 for the DE**C**A mutant.[55] As a test of the present calculations to predict and provide a physical basis for these changes, we evaluated how the $K^+ \rightarrow Na^+$ exchange free energies in Figure 5a would change when $-NH_3^+$, modeling the Lys side chain, was replaced by (1) a neutral amide group, $-CON(CH_3)_2$, mimicking the peptide backbone or the Asn/Gln side chain (Figure 6b), (2) a positively charged guanidinium moiety, $-NH(C{=}NH_2^+)NH_2$, mimicking the Arg side chain (Figure 6a), and (3) a negatively charged carboxylate group, $-COO^-$, mimicking the Asp/Glu side chain (Figure 6c).

The results in Figure 6 show that the calculations on model filter mutants reproduce the experimentally observed changes in $Na^+/K^+$ selectivity qualitatively. Compared to the $\Delta G^x$ ($x$ = 4−20) in the model DE**K**A filter (−7 to −8 kcal/mol, Figure 5a), those in the model mutant filters indicate that the selectivity

for $Na^+$ is (1) greatly diminished in the model DE**Q**A mutant (less negative $\Delta G^x \sim -2$ kcal/mol, Figure 6b), (2) nearly lost in the model DE**R**A mutant ($\Delta G^x \sim -1.0$ kcal/mol, Figure 6a), and (3) reversed in the model DE(**D**/**E**)A mutant (positive $\Delta G^x$, Figure 6c).

The fully optimized structures of the model wild-type and mutant filters provide a physical basis for these changes. Although the model DE**R**A mutant (**6a**) retains the tricoordinate ligand binding and hydrogen-bonding pattern of its wild-type DE**K**A counterpart (**5a**), the size of its pore, due to the larger dimension and specific chemical structure of the guanidinium group, is wider and probably less rigid than that of the DE**K**A filter: The sum of the distances between the three metal-bound O atoms is 11.4 Å for the model DE**R**A mutant (**6a**) but 10.6 Å for the wild-type filter (**5a**). As discussed above, a larger and more flexible pore is associated with a decrease in its $Na^+/K^+$ selectivity.

In contrast to the model DE**R**A mutant (**6a**), the metal cation in the carbonyl (**6b**) and carboxylate (**6c**) mutants is tetracoordinated, which, in line with the findings from the preceding sections (see also Table 1), decreases the $Na^+/K^+$ selectivity. Compared to the two-carboxylate filter **6b**, the increased negative charge density around the small $Na^+$ cation in the three-carboxylate structure **6c** further destabilizes the $Na^+$-bound pores relative to the $K^+$-bound pores to such an extent that $Na^+/K^+$ selectivity becomes reversed (Figure 6c). The increase in the $\Delta G^x$ in going from the two-carboxylate filter **6b** to the 3-carboxylate filter **6c** is consistent with the increase in the $\Delta G^x$ in going from filter3-$CONHCH_3(COO^-)_2$ (Figure 2d) to filter3-$(COO^-)_3$ (Figure 2e).

**Dynamic Model of Metal Selectivity.** Lipkind and Fozard[60,61] have hypothesized that the metal selectivity of $Na^+$ channels with the DEKA motif arises from the difference between the Lewis acidity of $Na^+$ and $K^+$, which allows $Na^+$, but not $K^+$, to successfully compete with the Lys $NH_3^+$ moiety for the negatively charged Asp and Glu side chains (see Introduction). To verify this hypothesis, the structures of the metal-free and metal-occupied model DEKA pores were fully optimized and the free energies of $Na^+/K^+$ binding to the pore were computed. Two cases were considered for the metal-free filters: a completely dehydrated pore (**7a**) and a partially hydrated structure (**7b**), suggested by Lipkind and Fozard's modeling studies.[60,61] In the fully dehydrated pore (**7a**), the Lys side chain hydrogen bonds to both carboxylate side chains. In the partially hydrated pore (**7b**), Lys interacts directly only with the adjacent acidic residue (Glu) but indirectly with the other carboxylate (Asp) via a water molecule. Our calculations reveal that the pore undergoes significant geometrical changes upon metal binding (Figure 7): Binding of $Na^+$ or $K^+$ in the pore pushes the Lys side chain away from the pore center. The Lys $NH_3^+$ group transfers a proton to the adjacent carboxylate (Glu) but loses its hydrogen bond with the opposite carboxylate (Asp) and forms a new hydrogen bond with the Ala backbone carbonyl O.

Contrary to the hypothesis of Lipkind and Fozard, both $Na^+$ and $K^+$ can displace the Lys side chain from the center of the pore and bind favorably to the filter's coordinating groups, as evidenced by the large negative binding free energies in the protein environment in Figure 7. $Na^+$ binding to a fully/partially dehydrated pore is more favorable than $K^+$ binding (by $\sim$7$-$8 kcal/mol); e.g., the $\Delta G^4/\Delta G^{20}$ for $Na^+$ binding to a partially dehydrated pore ($-58/-49$ kcal/mol) is more favorable than that for $K^+$ binding to the same pore ($-51/-41$ kcal/mol). This is due mostly to the specific physicochemical and mechanistic properties of the metal-occupied pores (constricted pore lined with three strong ligating groups) rather than to the different Lewis acidities of $Na^+$ and $K^+$ influencing the course of metal binding.

## Discussion

**Factors Governing the $Na^+/K^+$ Selectivity in Sodium Channels.** To the best of our knowledge, this work is the first attempt to systematically assess the effects of various factors involving properties of the native ion, the metal$-$ligands, and the protein matrix in determining the competition between $Na^+$ and $K^+$ in binding to $Na^+$ channels. The results reveal that the $Na^+$ channel's selectivity for $Na^+$ over $K^+$ increases if (1) the pore provides three rather than four protein ligands to coordinate to the metal ion, (2) the protein ligands have strong charge-donating ability such as Asp/Glu carboxylate or backbone carbonyl groups, (3) the pore is relatively narrow, rigid, and solvent exposed, and (4) the passing $Na^+$ is bare or less well hydrated than the competing $K^+$ inside the filter. It also reveals the physical basis of the observed trends, which are consistent with available experimental data, as discussed below.

**Number of Protein Ligands.** Our calculations suggest that selectivity filters lined with fewer protein ligands are more selective for $Na^+$, as this reduces the steric repulsion among the bulky protein ligands around the small $Na^+$ more than that around the larger $K^+$ (see Table 1). Selectivity filters lined with three protein ligands appear to be optimal for $Na^+$ channels. Indeed, the family of degenerin/epithelial $Na^+$ channels has been shown to have trimeric structure.[41,42] Even though the voltage-gated $Na^+$ channel with the DEKA selectivity filter has an overall tetrameric structure, our results show that the metal ion is in fact coordinated to only three of the conserved residues comprising the DEKA motif: the Lys side chain, which forms a hydrogen bond network with the other metal ligands, does not directly coordinate with the metal cation (Figure 5). That $Na^+$ prefers to coordinate to three rather than four protein ligands is also supported by the fact that "DE**X**A" mutants donating four protein ligands to the metal cation have greatly diminished or even reversed $Na^+/K^+$ selectivity (Figure 6b,c).

**Ligating Strength of Protein Ligands.** In line with previous predictions,[20] increasing the ligating strength of the coordinating groups enhances $Na^+/K^+$ selectivity, since a ligand with higher field strength provides more favorable interactions with $Na^+$ than the larger $K^+$, thus helping to offset the larger $Na^+$ dehydration penalty. This provides a rationale for the presence of Asp/Glu in the DEKA selectivity filter of the voltage-gated $Na^+$ channels, as negatively charged carboxylates can significantly increase the $Na^+/K^+$ selectivity of the pore (see Figure 2). Note that the Na1 binding site of the LeuT transporter also utilizes the negatively charged carboxylate of the metal-bound leucine substrate to attain high $Na^+$ over $K^+$ selectivity.[68,81]

**Size/Rigidity of the Pore.** The results herein reveal that the size/rigidity of the pore plays a more important role in determining the $Na^+$ vs $K^+$ selectivity in $Na^+$ channels than in $K^+$ channels. This is mainly because a narrow and constricted pore in $Na^+$ channels is more discriminative toward larger cations ($K^+$) than the larger aperture in $K^+$ channels is toward smaller cations ($Na^+$) (see Results). This finding also helps to explain why the highly selective voltage-gated $Na^+$ channels have evolved to possess a DEKA selectivity filter where the Lys is required for $Na^+/K^+$ discrimination: The Lys side chain

(81) Yamashita, A.; Singh, S. K.; Kawate, T.; Jin, Y.; Gouaux, E. *Nature* **2005**, *437*, 215–223.

helps to constrict and rigidify the pore by forming a tight hydrogen-bond network with neighboring coordinating groups, so any deviations from the pore's optimal size/rigidity result in decreased $Na^+$ selectivity (compare **5a** and **6a**). The role of the Lys side chain in stabilizing the channel pore is in accord with previous works.[55,57,58,80] Along a similar vein, the Na2 binding site of the LeuT transporter lined with several neutral ligands achieves high $Na^+/K^+$ selectivity due to the structural stiffness of the site imposed by an elaborate local hydrogen-bond network and covalent connectivity.[68]

**Solvent Exposure of the Pore.** Recent studies suggest a relationship between the dielectric constant of the environment and the $K^+$ HN: increasing the solvent exposure of the pore (increasing $\varepsilon$) favors a lower $K^+$ HN.[31,33] Thus, the physico-mechanical properties of the pore may affect the metal HN inside the channel and, respectively, its selectivity. As our calculations suggest, pores supporting lower $K^+$ HNs in the vicinity of the selectivity filter are expected to be more selective for $Na^+$ (Table 1).

**Partial Hydration and Coordination Number of the Metal Inside the Filter.** Our calculations suggest that in trimeric filters lined with neutral ligating groups, complete dehydration of both metal cations enhances $Na^+/K^+$ selectivity (compare Figure 2a,b with Figure 3a,b). Partial cation hydration inside the filter increases the metal CN, which generally disfavors the $Na^+/K^+$ selectivity in pores lined with low ligating-strength groups such as $-$OH from Ser/Thr side chains. This is in line with the above finding that increasing the number of protein ligands from three to four also disfavors $Na^+/K^+$ selectivity (Table 1). Thus, in selectivity filters of epithelial $Na^+$ channel, which are devoid of negatively charged aa residues, the number of protein (as opposed to water) ligands as well as the stiffness and solvent exposure of the pore appear to be the key determinants of the $Na^+$ selectivity (see above).[72]

**Comparison Between the Determinants of Metal Selectivity in $K^+$ and $Na^+$ Channels.** Although the voltage-gated $Na^+$ channels have similar overall structure to the voltage-gated $K^+$ channels and are thought to have evolved from $K^+$ channels by gene duplication,[2] the composition and architecture of their selectivity filters appear different from those of their $K^+$ channel counterparts: The selectivity filter of the voltage-gated $Na^+$ channel appears to be a single-layered asymmetrical ring with aa side chains contributing to the metal selectivity, whereas the selectivity filter of the voltage-gated $K^+$ channel consists of four homotetrameric rings, one on top of the other, lined with backbone carbonyl groups.[10] The difference in the selectivity filters' composition and structure implies different mechanisms/principles of metal selectivity for $Na^+$ and $K^+$ channels.

Indeed, the present results in combination with previous studies on $K^+$ channels[15,20−34] reveal that factors favoring $K^+/Na^+$ selectivity in $K^+$ channels generally disfavor $Na^+/K^+$ selectivity in $Na^+$ channels and vice versa. The high $K^+/Na^+$ selectivity of $K^+$ channels can be achieved mainly by maximizing the $K^+$ HN and CN inside the pore, but minimizing the ligating strength of the metal−ligands.[34] Thus, high selectivity of $K^+$ over $Na^+$ in $K^+$ channels could be achieved by a relatively buried pore, which favors an octahydrated $K^+$, lined with eight coordinating weak dipoles as opposed to strong charge-donating carboxylate groups. Conversely, the high $Na^+/K^+$ selectivity of $Na^+$ channels can be achieved mainly by minimizing the $K^+$ HN and the protein ligands inside the pore but maximizing the ligating strength of the metal−ligands. Thus, high selectivity of $Na^+$ over $K^+$ in $Na^+$ channels could be achieved by a relatively solvent exposed pore, which favors a hexahydrated $K^+$, lined with only three protein ligands with strong ligating strength, such as backbone carbonyl groups and one or two Asp/Glu side chains. Additionally a constricted, rigid conducting pore also contributes to the $Na^+/K^+$ selectivity $Na^+$ channels.

**Biological Implications.** The results herein provide clues to the metal-binding site structure in the selectivity filter, in particular, the orientation of (i) the Ser side chains in epithelial $Na^+$ channels and (ii) the Ala side chain in voltage-gated $Na^+$ channels. Mutagenesis data on the epithelial $Na^+$ channel suggest that the hydroxyl O of the conserved Ser lining the asymmetric selectivity filter from the $\alpha$ subunit, but not from the $\beta$ and $\gamma$ subunits, plays a key role in conferring $Na^+/K^+$ selectivity.[49] However, the conserved Gly and Ser lining the selectivity filter from the $\beta$ and $\gamma$ subunits, respectively, are important in restricting $K^+$ permeation. On the other hand, our results show that a higher $Na^+/K^+$ selectivity is achieved by metal coordination to three rather than four protein ligands (Table 1) and carbonyl O rather than hydroxyl O (compare parts a and b of Figure 2). The combination of the experimental data and our computed free energies suggest that $Na^+$ is probably coordinated to a serine hydroxyl O and two backbone carbonyl O atoms lining a relatively narrow and rigid selectivity filter in epithelial $Na^+$ channels.

Along the same vein, the results in Figure 5 suggest that the Ala comprising the DEKA motif in voltage-gated $Na^+$ channels orients its backbone carbonyl O toward the pore lumen to bind the metal, in accord with previous work.[60,61] This is because $Na^+/K^+$ selectivity is high when the metal coordinates to the carbonyl O (from Ala) in addition to the two carboxylates (from Asp/Glu) (Figure 5a,b) but is abolished when it binds only the two carboxylates (Figure 5c). Our results also suggest that the Lys in the DEKA motif is likely protonated and forms hydrogen bonds with both the carbonyl O and carboxylate O to constrict and rigidify the pore (Figure 5a).

**Acknowledgment.** Support by the Institute of Biomedical Sciences, Academia Sinica, and the NSC contract no. NSC 95-2113-M-001-001 is appreciated.

**Supporting Information Available:** Complete refs 67 and 70 and Table S1. This material is available free of charge via the Internet at http://pubs.acs.org.

JA909280G